Hexa-Band Antenna for Smartphone Applications

[(1)]Saqer S. Alja'afreh, [(2)] Yi.Huang, [(3)]Qian.Xu, [(3)]Lei. Xing
[1] *Electrical Engineering Department, Mu'tah University, Alkarak, Jordan*
[2]*Department of Electrical Engineering & Electronics. University of Liverpool, United Kingdom*
[3] *Department of Electrical Engineering & Electronics, Nanjing University of Aeronautics and Astronautics Nanjing, China*
[(1)]saqer1981@yahoo.com, [(2)]Yi.Huang@liv.ac.uk, [(3)]emxu@foxmail.com, [(3)]xinglei@nuaa.edu.cn

Abstract—**A new low-profile metallic frame antenna is proposed for hexa-band Smartphone applications. It consists of two frame segments (Segment 1 as a main radiator and Segment 2 which acts as a wave trap). The main segment works as a shorted monopole antenna (PIFA-like antenna) with a modified shape. By combining different modes of the shorted monopole and loading stubs, a hexa-band operation is achieved. The antenna is analyzed and optimized in terms of the reflection coefficient and the current distribution. The final design is made and tested and the results show that this design covers a hexa-band and is particularly suitable for such as GSM850/ DCS1800/ PCS1900/ UMTS2100/ LTE2500/ LTE3600 mobile applications.**

***Index Terms*-Parasistic Decoupling Element; 4G, MIMO; PILA; Diversity Antenna.**

I. INTRODUCTION

Recently, Smartphones have dominated mobile markets and are still enjoying a rapid growth. A current trend in Smartphone design is to use a metallic frame in housing for adding more mechanical strength and nice cosmetic appearance [1]. Another advantage of the metallic frame lies in the integration with the antenna circuitry. Metal frame antennas are very attractive as they occupy a narrow space with the casing of portable devices; this can save more space for other handset components such as the large display, battery, etc.

In this context, several promising designs have been proposed. For example, a low-profile metal frame antenna was reported in [2] but lumped elements were used to provide impedance matching which affected the radiation efficiency. In [3-6], several multiband designs were proposed, but all of them shared the same drawback: the same chassis mode was used for frequencies below 1 GHz, which usually increases the difficulty of installing other handset antennas and made them not suitable for the recent MIMO technology. To overcome this problem, interesting design solutions have been reported in [7-8] where a new characteristic mode (orthogonal to the conventional chassis dipole mode below 1 GHz) has been excited by a metal frame antenna. This facilitated the introduction of a dual-element antenna for MIMO applications. However, these proposed solutions are high profile designs and can only cover single band [7] or dual band [8].

To alleviate these drawbacks, a new, low profile hexa-band metal frame antenna is proposed. It combines the resonance modes created by a metal frame (dual-branch shorted monopole) and its loading stubs. A detailed evolutionary process is carried out, which shows the operational mechanism of the proposed antenna. Overall, the proposed solution can cover six bands for cellular radios. Hence it is a very promising candidate for mobile portable devices.

The organization of this letter is arranged as follows: In Section II, the antenna geometry and the design process are presented. The antenna prototype, the simulation and measurement results are presented in Section III. Finally, the conclusion is drawn in Section IV.

II. ANTENNA DESIGN AND DESIGN PROCESS

(A) Antenna Configuration

The geometry of the proposed frame antenna is depicted in Fig. 1 with the optimized dimensions. The design uses a *1 mm* thick FR4 substrate of dimensions $60\times130\ mm^2$ relative permittivity *4.4* and loss tangent *0.025* as the system printed circuit board (PCB) and the substrate material for the metal frame antenna. The metal frame is composed of two parts segment 1 (the main radiator) and segment 2. For ease of fabrication, each segment is printed on a *1 mm* thick FR4 substrate of dimensions $8\times130\ mm^2$. Unlike [7-8] that have high profiles (8 mm height above PCB), the frame is positioned vertically, next to the system PCB with *4 mm* above and *4 mm* below the ground plane; this will keep the total thickness of the resulting handset device within the limit (Thickness ≤ 8 *mm*), even after the integration of both the LCD display and the battery. The gaps between the ground plane and the frame antenna segments are *3.5 mm* and *1 mm* from segment 1 and segment 2, respectively. The area without the ground at the top edge of the PCB is $60\times13\ mm^2$; this cleared area can be used to install another antenna element as it will excite the conventional dipole chassis mode below 1 GHz [7, 8] and this will simplify the design of MIMO antenna. A narrow plate parallel ($3\times20\ mm^2$) to the system PCB, is used to create a capacitive coupling that can excite the frame mode properly. It is connected to segment 1 and fed by a vertical feeding plate connected to a feeding probe (not shown for the clarity of the figure). As shown by Fig. 1(b), the feeding plate is placed at a *60 mm* from the top edge of the PCB with dimensions $4\times10\ mm^2$; also the shorting plates (Short 1 and Short 2) with dimensions 4×5 mm^2 are used to connect the frame segments to the ground plane. Fig.1(c) shows the detailed dimensions of the main segment. The frame is loaded with stubs to provide the multiband operation. Segment 2 (see Fig. 1(d)) is added to enhance the operational bandwidth at the lower frequency band (GSM850).

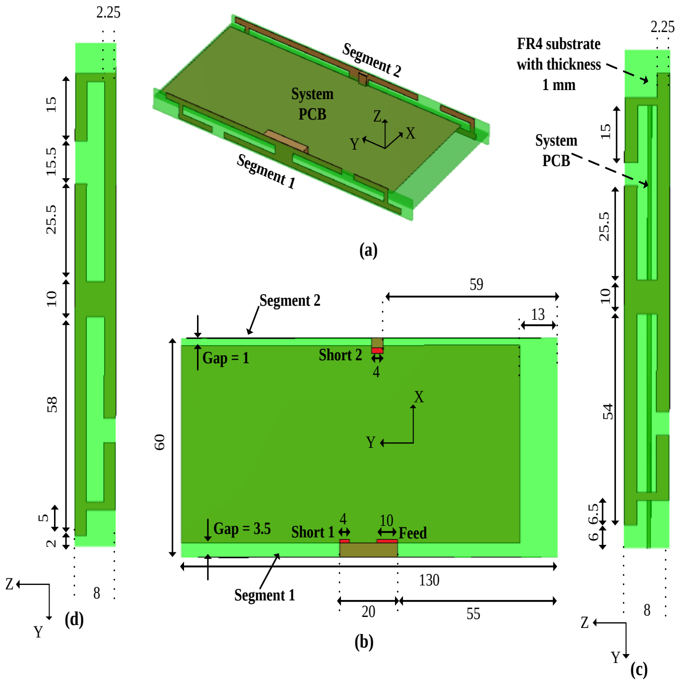

Fig. 1. Geometry of the proposed design: (a) 3D antenna geometry, (b) the top view with detailed dimensions, (C) Segment 1 with detailed dimensions and (d) Segment 2 with detailed dimensions. (Unit: mm)

B. Design Process

To reveal the operational mechanism of the proposed antenna, an evolutional design process, including four stages, is shown in Fig. 2 (a) and the resulted reflection coefficient S11 after each design stage is presented in Fig. 2 (b). Initially, the design was like a dual-branch shorted monopole as shown in Stage I. It is clearly shown that the design in Stage I has three resonance modes at 0.99 GHz, 2.1 GHz and 3.18 GHz, corresponding to the 0.25 λ (branch #1), 0.25 λ (branch #2) and 0.75 λ (branch #1), respectively. Stub 1 (inverted-L shape) was added in Stage II for two reasons: the first one is to provide an inductive loading for branch #1 resonance modes (0.25 λ and 0.75 λ), both were shifted down to 0.85 GHz and 2.55 GHz. The second one is to create a new resonant frequency at the higher frequency bands, this can be seen from Fig. 2(b) where a new resonance deep appears at 3.75 GHz which is linked to 0.25 λ mode of the Stub. In order to achieve a wideband operation in the frequency range 1.7 GHz to 2.2 GHz, a new resonance mode (f = 1.85 GHz) was created in Stage III by the addition of Stub 2 (0.25 λ), it was tuned to 1.85 GHz to merge with 2.1 GHz resonance. Thus, DCS1800, PCS1900 and UMTS2100 all were covered by Stage 3 as shown in Fig. 2(b). It is worth mentioning that the rest metallic part of segment 1 was added to provide more mechanical strength and a nice appearance. Finally, the second frame segment (segment 2) was added in Stage IV to work as a wavetrap that can enhance impedance bandwidth at 0.85 GHz as shown in Fig. 2(b). Thus, for the 6-dB return loss bandwidth, the design covers six frequency bands ranging from GSM850 to LTE3600.

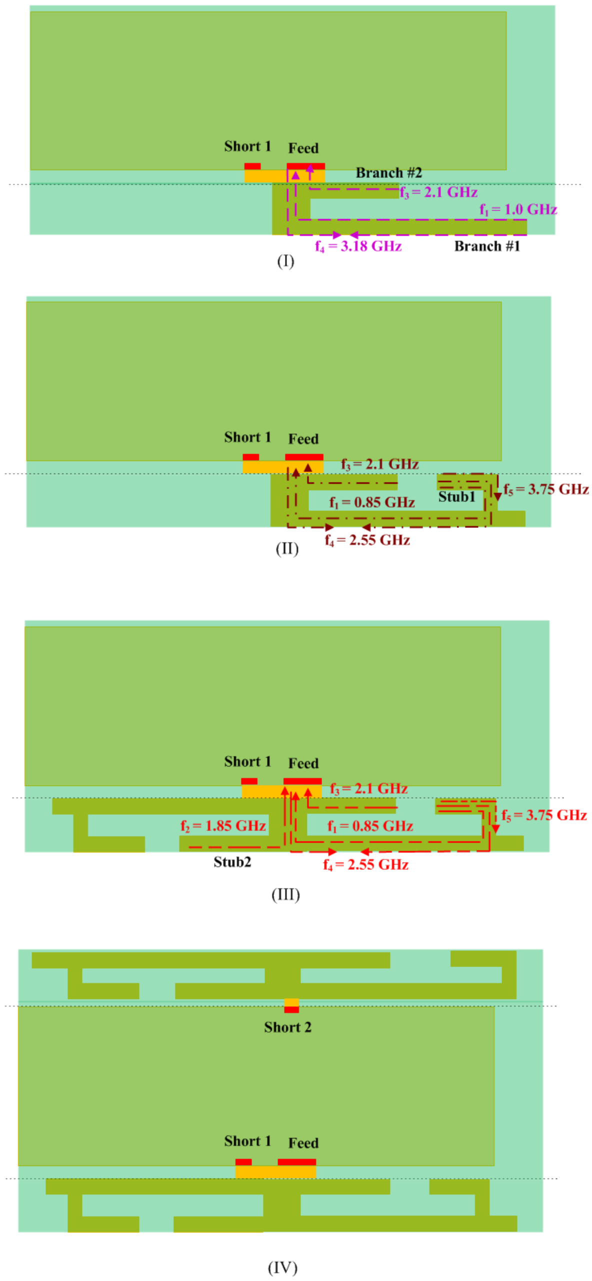

(a)

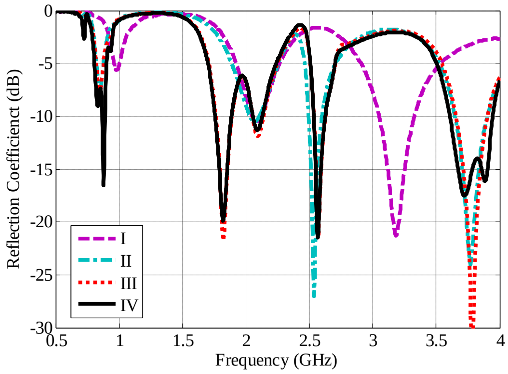

(b)

Fig. 2. (a) The step by step change on the frame geometry (planar form) and (b) S_{11} evolutions

To further understand the multiband operation, simulated surface current distributions at five resonant frequencies are given in Fig. 3. Obviously, for the lowest frequency band (0.85 GHz), the largest surface current density is observed along the frame segments, which represents 0.25 λ PIFA-like fundamental mode. It can be seen also how is the chassis current is trapped by segment 2, which helps in enhancing the impedance bandwidth. For the second (1.85 GHz) and third (2.1 GHz) resonances, the current distributions become more concentrated on Stub 2 and branch #2, respectively, Both of them represent 0.25 λ resonance modes (see Fig. 3(b) and (c)). For the higher resonant frequencies, it is clearly shown by Fig. 3 (d) that the resonance at 2.55 GHz is linked to the 0.75 λ resonance of branch #1 while at 3.7 GHz it is related to 0.25 λ Stub 1 (inverted-L) mode.

III. Simulated and Measured Results

Simulations were performed using CST Microwave Studio to optimize the antenna parameters for the desired frequency bands. A prototype of the optimised design (shown in Fig. 4) was fabricated and tested. Fig. 5 shows the measured and the simulated reflection coefficients. A good agreement can be seen, a small discrepancy between them in the high frequency bands is due the effect of soldering and structure assembling. Based on the 6 dB return loss bandwidth, the proposed frame antenna covers six operating bands which are GSM850/ DCS1800/ PCS1900/ UMTS2100 /LTE2500/ LTE3600.

Fig. 6 shows the simulated and measured normalized radiation patterns of the proposed antenna. It can be seen the big advantage of this design over other multiband designs [3-6] at the lower frequency 0.85 GHz, the design has orthogonal patterns to the common and conventional chassis mode; also this can be understood from the 3D simulated radiation pattern at 0.85 GHz as shown in Fig. 7. This can facilitate the design of an MIMO antenna below 1GHz. As mentioned earlier, this design presents a multiband solution over [7, 8], the radiation patterns at the higher resonance frequencies are also included in Fig. 7. The simulated and the measured results are in good agreements, slight difference occurs in higher frequency results, which corresponds to the feeding cable and the orientation (some inclination may exist) of the antenna during the measurement, especially, on the vertical planes (XZ and YZ planes).

Finally, the total efficiency of the fabricated antenna was measured inside our reverberation chamber. Table I shows the measured and simulated total efficiency obtained at resonant frequencies 0.85, 1.8, 2.1, 2.55 and 3.75 GHz. The results are in a good agreement (the measured ones are slightly smaller) and the discrepancy between the results is likely due to the fabrication errors and the material property variations.

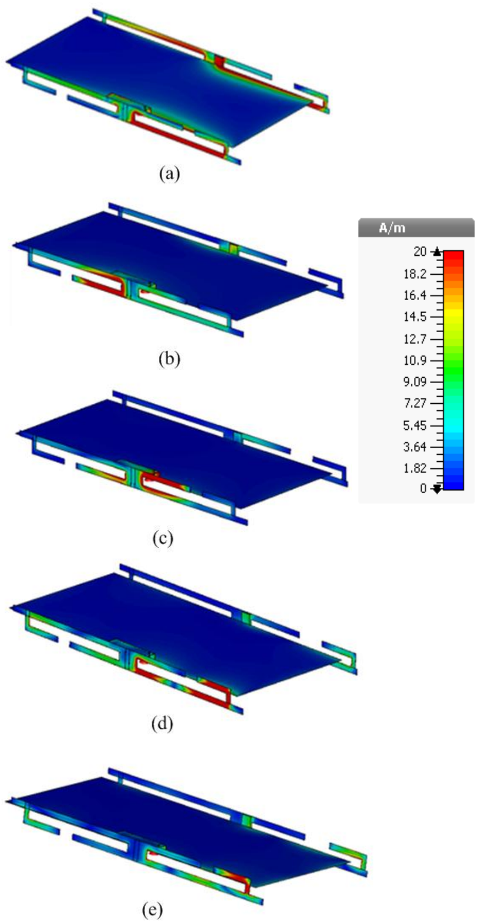

Fig. 3. Simulated surface current distributions (a) 0.85 GHz, (b) 1.85 GHz, (c) 2.1 GHz, (d) 2.55 GHz and (e) at 3.75 GHz.

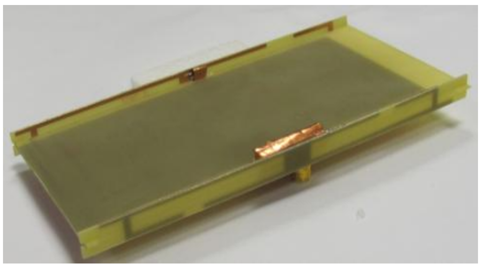

Fig. 4. The fabricated prototype

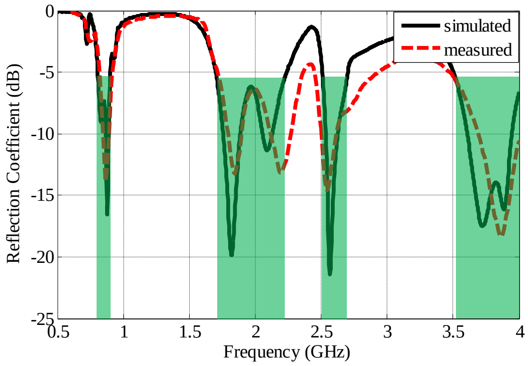

Fig. 5. Measured and simulated reflection coefficients

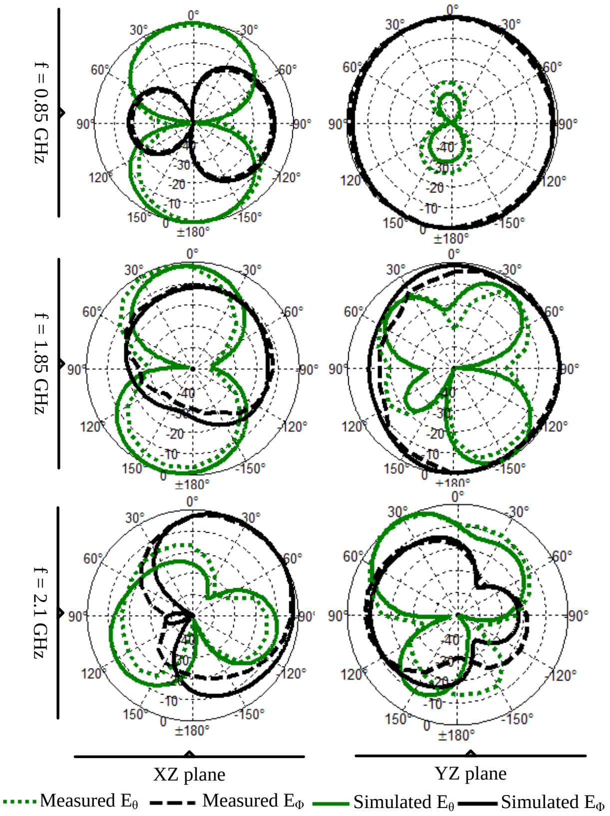

Fig. 6. Measured and simulated normalized radiation patterns

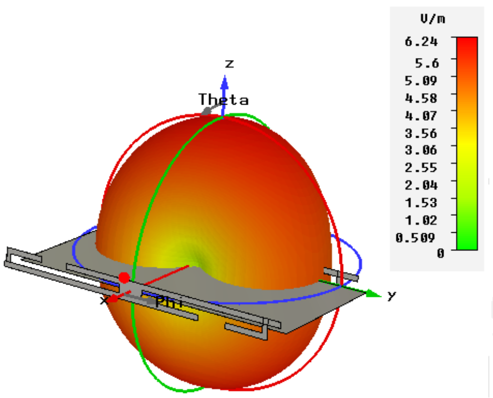

Fig. 7. 3D simulated far field pattern at 0.85 GHz

TABLE I
MEASURED AND SIMULATED TOTAL EFFICIENCY

Frequency (GHz)	Simulated	Measured
0.85	83%	79%
1.8	90%	82%
2.1	85%	80%
2.55	87%	82%
3.75	86%	83%

IV. CONCLUSIONS

A new, simple and low-profile hexa-band frame antenna has been proposed for multiband mobile applications. The multiband operation has been achieved using a modified metal frame that is loaded with two kinds of stubs. The working mechanism and the design principle of the antenna have been presented in a simplified way. A prototype has been designed, fabricated and measured. The results have shown that the design can cover six frequency bands with S_{11}< -6 dB. Furthermore, the design presents a multiband metal frame antenna solution that depends on an orthogonal mode, especially, for frequencies below 1 GHz, which in turns simplifies the implementation of MIMO antennas for such applications. Thus, the integration of this hexa-band metallic frame antenna with another antenna element on the top edge is under investigation.

REFERENCES

[1] J. Anguera, A. Andújar et al, "Advances in Antenna Technology for Wireless Handheld Devices ," Internaltiona Journal on Antenna and Propoagation., vol. 2013, Article ID: 838364, 2013.

[2] Y. L. Ban, Y. F. Qiang, Z. Chen, K. Kang and J. L. Wei-Li, "Low-Profile Narrow-Frame Antenna for Seven-band WWAN/LTE Smartphone Applications ," *IEEE Antenna Wireless Propag. Lett.*, vol. 13, pp. 463-466, 2014.

[3] L. W. Zhang and Y. L. Ban, "Novel Hepta-band Coupled-Fed Antenna for WWAN/LTE Metal-Ring-Frame Smartphone Applications ," *PIERS Proceeding.*, pp. 2190–2193. 2014.

[4] J. Zhong, K. K. Chen and X. Sun, "A Novel Multi-band Antenna for Mobile Phone with Metal Frame," *in Proc. 8th International Conference on Wireless Communications, Networking and Mobile Computing (WiCOM)*, Sept. 2012, China.

[5] S. Eom, M. Ali, S. O. Park and H. Kim, "Embedded Antenna for Metallic Handheld Communication Devices," *Progress in Electromagnetics Research B.*, vol. 57, pp. 127-138, 2014.

[6] Y. L. Ban, Y.F. Qiang, Z. Chen *et al*, "A Dual-Loop Antenna Design for Hepta-Band WWAN/LTE Metal-Rimmed Smartphone Applications," *IEEE Trans. Antennas Propag.*, vol. 63, no. 1, pp. 48-58, 2015.

[7] H. Li, Z. Miers and B. K. Lau., "Design of Orthogonal MIMOHandset Antennas Based on Characteristic Mode Manipulation at Frequency Bands Below 1 GHz," *IEEE Trans. Antennas Propag.*, vol. 62, no. 5, pp. 2756-2766, 2014.

[8] Z. Miers, H. Li and B. K. Kiong., "Design of Bandwidth-Enhanced and Multiban MIMO Antennas Using Charaterisitcs Modes," *IEEE Antenna Wireless Propag. Lett.*, vol. 12, pp. 1696-1699, 2013.